The Folding Landscape of an α-Lytic Protease Variant Reveals the Role of a Conserved β-Hairpin in the Development of Kinetic Stability

Stephanie M. E. Truhlar[1†] and David A. Agard[1,2*]

[1]*Graduate Program in Chemistry and Chemical Biology, University of California, San Francisco, San Francisco, California*

[2]*Howard Hughes Medical Institute and the Department of Biochemistry and Biophysics, University of California, San Francisco, San Francisco, California*

ABSTRACT **Most secreted bacterial proteases, including α-lytic protease (αLP), are synthesized with covalently attached pro regions necessary for their folding. The αLP folding landscape revealed that its pro region, a potent folding catalyst, is required to circumvent an extremely large folding free energy of activation that appears to be a consequence of its unique unfolding transition. Remarkably, the αLP native state is thermodynamically unstable; a large unfolding free energy barrier is solely responsible for the persistence of its native state. Although αLP folding is well characterized, the structural origins of its remarkable folding mechanism remain unclear. A conserved β-hairpin in the C-terminal domain was identified as a structural element whose formation and positioning may contribute to the large folding free energy barrier. In this article, we characterize the folding of an αLP variant with a more favorable β-hairpin turn conformation ($\alpha LP_{\beta\text{-turn}}$). Indeed, $\alpha LP_{\beta\text{-turn}}$ pro region-catalyzed folding is faster than that for αLP. However, instead of accelerating spontaneous folding, $\alpha LP_{\beta\text{-turn}}$ actually unfolds more slowly than αLP. Our data support a model where the β-hairpin is formed early, but its packing with a loop in the N-terminal domain happens late in the folding reaction. This tight packing at the domain interface enhances the kinetic stability of $\alpha LP_{\beta\text{-turn}}$, to nearly the same degree as the change between αLP and a faster folding homolog. However, $\alpha LP_{\beta\text{-turn}}$ has impaired proteolytic activity that negates the beneficial folding properties of this variant. This study demonstrates the evolutionary limitations imposed by the simultaneous optimization of folding and functional properties. Proteins 2005;61:105–114.**

Key words: α-lytic protease; pro region; protein folding; kinetic stability; β-hairpin

INTRODUCTION

Nearly all secreted bacterial proteases are synthesized with N- or C-terminal pro regions that are required to facilitate their folding.[1–3] Characterization of the folding of α-lytic protease (αLP),[4–6] one of the best studied members of this class of proteins, revealed that in the absence of its pro region the isolated protease domain folds extremely slowly [$t_{1/2}$ ~1700 y; Fig. 1(a)].[4,7] Rapid folding of αLP only occurs in the presence of its pro region (Pro), which accelerates folding by a factor of ~10^9.[4,6] Following formation of the native state, Pro is degraded, releasing the active protease.[8] Remarkably, the native state of αLP is thermodynamically less stable than both the fully unfolded molecule and a molten-globule folding intermediate. Instead, the αLP native state is stabilized kinetically; a large free energy of activation for unfolding ($t_{1/2}$ ~1 y) is solely responsible for the persistence of the native state.[4,7,9]

The generality of this folding mechanism was revealed by the folding landscape of *Streptomyces griseus* protease B (SGPB), a homolog of αLP [Fig. 1(b)].[7] Both proteases are characterized by large free energies of activation for folding, surmounted only with the assistance of their pro regions, and large free energies of activation for unfolding, from which the proteins derive their kinetic stability. However, SGPB, which folds with a smaller, less effective pro region, has smaller free energies of activation for both folding and unfolding. The size of the pro region seems to correlate not only with its efficacy as a folding catalyst, but it also serves as an indicator of the magnitude of the folding free energy barrier.[7]

The kinetic stability of αLP and SGPB, and presumably all pro-proteases, allow them to attain an extraordinary functional advantage. As extracellular bacterial proteases, αLP and SGPB degrade proteins to provide nutrients for their host organisms, and therefore function in a highly proteolytic environment. Thus, there is an evolutionary advantage for these enzymes to optimize their resistance to proteolytic destruction. Proteases require their substrates to be conformationally flexible, for example, to have loops or unfolded conformations, for efficient sub-

Grant sponsor: a National Science Foundation Predoctoral Fellowship (to S.M.E.T.)

Grant sponsor: the Howard Hughes Medical Institute

†Current address (S.M.E.T.): Department of Chemistry and Biochemistry, University of California, San Diego, La Jolla, CA.

*Correspondence to: David Agard, University of California, San Francisco, 600 16th St. Rm. S412D, San Francisco, CA 94143-2240. E-mail: agard@msg.ucsf.edu

Received 16 November 2004; Accepted 10 February 2005

Published online 25 July 2005 in Wiley InterScience (www.interscience.wiley.com). DOI: 10.1002/prot.20525

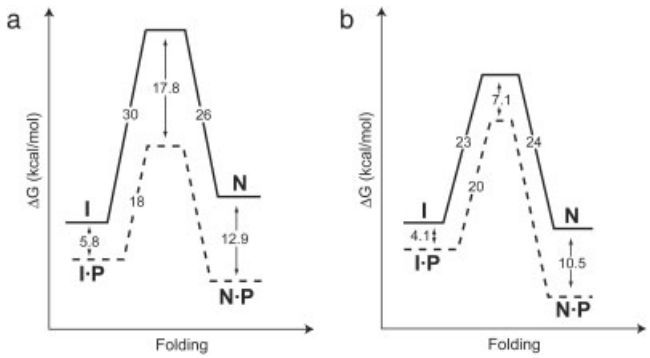

Fig. 1. Folding landscapes for αLP and SGPB at 0°C. Solid lines depict the free energies of activation for folding and unfolding encountered by αLP (**a**) and SGPB (**b**). Dashed lines illustrate the effect of their respective pro regions (P) on their folding profiles. The native state (N) of αLP is less thermodynamically stable than its intermediate state (I). In contrast, the native state of SGPB is marginally stable compared to its intermediate state. Free energies of activation were calculated from folding and unfolding rates using transition state theory.[48] The affinities of their pro regions for the αLP and SGPB native states were measured at 25°C.

strate binding and cleavage.[10–13] αLP and SGPB have suppressed all local unfolding events[7,9] that are typical of most proteins,[14–16] such as partial unfolding of subdomains or small fluctuations around the native structure (breathing motions). The extremely cooperative nature of their unfolding transitions results in reduced sensitivity to exogenous proteolysis and extended functional lifetimes for αLP and SGPB, compared to typical, thermodynamically stable proteins that fold independently, such as trypsin.[17] In fact, when αLP, SGPB, and trypsin are mixed together in a protease survival assay, αLP and SGPB outlast trypsin by factors of ~20 and ~8, respectively.[7]

Although the kinetic stability of αLP and SGPB gives these proteins an important functional advantage, it comes with large costs for folding and stability. An increase in protease resistance by a factor of ~2.4–8 comes with a cost of a factor of $\sim 10^5$ in the spontaneous folding rate, and a loss of 5–10 kcal/mol of native state thermodynamic stability.[7] Overcoming these penalties has necessitated the coevolution of increasingly effective pro region folding catalysts. This decoupling of the folding and native landscapes has allowed these proteases to attain native-state properties that traditional proteins, subject to concurrent evolutionary pressures on folding and function, cannot reach.

Although the folding landscapes are well characterized, the structural origins of these unique folding properties remain unclear. The crystal structure of Pro bound to the αLP native state revealed that an extended β-hairpin (αLP residues 118–130) pairs with a three-stranded β-sheet in the pro region to form a continuous five-stranded β-sheet in the complex [Fig. 2(a)] (all αLP and SGPB residue numbering is sequential).[18] This suggested that the pro region might play an important role in forming and correctly positioning the β-hairpin. This β-hairpin is conserved among all proteases of the chymotrypsin superfamily that are associated with pro regions, but is replaced by different structures or absent in homologs that fold independently of their short zymogen peptides.[18] Furthermore, two variants of αLP with alterations in the β-hairpin (V119I and N122K) reduced the efficiency of pro region folding catalysis, both in initial binding to the intermediate state and stabilization of the folding transition state.[19] Additionally, a screen for faster folding variants of αLP resulted in a double mutant (R102H/G134S), located at the top of the β-hairpin, whose spontaneous folding is 370 times faster than WT αLP.[20]

Although the β-hairpin is conserved in both αLP and SGPB, the conformation of the β-hairpin turn differs between the two proteins [Fig. 2(b)]. A primary sequence alignment of homologous pro-proteases indicated that the conformation of the β-hairpin turn covaries with pro region size. All proteases associated with short pro regions adopt type I′ or type II′ turn geometries, while long pro region-containing proteases adopt type I turns.[21] A detailed survey of β-hairpin structures in 63 proteins revealed that type I′ and type II′ β-turns are the predominant conformations observed in β-hairpins.[21] It was proposed that these turn conformations are more compatible with the natural right-handed twist of the antiparallel β-sheet.[22,23] Type I turns are far less frequent and may be less stable in β-hairpins.[21,24] Peptide studies have shown that a favorable turn conformation can contribute ~0.5–1 kcal/mol of stability to the β-hairpin.[25,26] Overall, this suggests that the conformation of the β-hairpin turn in αLP is less stable than that found in SGPB, which may contribute to the larger free energy of activation for folding encountered by αLP.

To determine whether the conserved β-hairpin is a key structural element involved in the large folding free energy barrier encountered by the pro-proteases, we tested the role of the β-hairpin in the folding landscape of αLP by replacing its turn with the more favorable turn sequence from SGPB ($\alpha LP_{\beta\text{-turn}}$). Surprisingly, we find that the more favorable β-turn conformation results in an increase in kinetic stability, rather than the expected faster folding. However, this functional advantage is offset by the lower proteolytic activity of the $\alpha LP_{\beta\text{-turn}}$ variant. The role of the β-hairpin begins to elucidate the structural origins of kinetic stability and also highlights the evolutionary restrictions that result from the simultaneous optimization of folding and functional properties.

MATERIALS AND METHODS

$\alpha LP_{\beta\text{-turn}}$ Construct

To assess the impact of the β-hairpin turn conformation on αLP folding, a mutant αLP ($\alpha LP_{\beta\text{-turn}}$) was created where its β-hairpin turn (residues 124–127: AEGA)[27] was replaced with that from SGPB (residues 122–126: GGGDV).[28] The plasmid pAlp12BamHI[29] was digested with AgeI and EcoNI to remove a 75 base pair fragment containing the β-hairpin turn. An oligonucleotide cassette (MWG Biotech, Inc.) containing the SGPB β-hairpin turn sequence was ligated into the resulting AgeI- and EcoNI-digested plasmid, and was verified by double-stranded sequencing (MWG Biotech, Inc.).

Fig. 2. Crystal structure of αLP bound to its pro region. (**a**) The crystal structure of the native state of αLP is shown in blue (N-terminal domain in light blue, C-terminal domain in dark blue), with the conserved β-hairpin (residues 118–130) shown in cyan and the side chains of the catalytic triad (His36, Asp63, and Ser143) shown in red. The pro region, shown in green, binds to the C-terminal domain of the protease, with a three-stranded β-sheet in the pro region pairing with the conserved β-hairpin in the protease and the pro region C-terminal tail inserted into the protease active site. (**b**) A detailed stereo view of the β-hairpin from the native αLP structure bound to its pro region from panel a, with an aligned crystal structure of the SGPB β-hairpin shown in pink. The β-hairpin turn residues (αLP residues 124–127: AEGA;[27] SGPB residues 122–126: GGGDV[28]) are shown with ball-and-stick representation. The backbone of the loop in the αLP N-terminal domain (residues 59–62) that contacts the β-hairpin, and the F59 and P60 side chains, are also shown with ball-and-stick representation. The SGPB V126 geometry appears to be aligned such that the A127V substitution in $\alpha LP_{\beta\text{-turn}}$ could pack with W119 in the pro region to enhance the affinity of Pro for this variant. The SGPB D125 geometry appears to be situated such that the G126D substitution could pack with αLP residues F59 and P60 in the N-terminal domain loop in the $\alpha LP_{\beta\text{-turn}}$ variant. Figure prepared using PyMOL v. 0.97.[49]

WT αLP and $\alpha LP_{\beta\text{-turn}}$ Production and Purification

Wild-type αLP was produced in liquid cultures of *Lysobacter enzymogenes* 495 (ATCC 29487),[30] purified,[31] and denatured[20] as described previously.

$\alpha LP_{\beta\text{-turn}}$ was expressed with Pro, as a single continuous polypeptide chain, in *Escherichia coli* strain D1210[32] as described previously.[33] The protein was partially purified by cation exchange chromatography as described previously,[31] except that the protein was washed and eluted at pH 8.4. Any Pro that remained bound to the protease was removed by treatment of the pooled $\alpha LP_{\beta\text{-turn}}$-containing fractions with pepsin as described previously.[29] Further purification was achieved by Mono-S (Pharmacia) HPLC, as described previously.[31] A portion was denatured as described previously.[20] Protein purity was verified by MALDI mass spectrometry. The concentration of $\alpha LP_{\beta\text{-turn}}$ was determined by absorbance measurements (280 nm) and dye binding.[34,35]

Pro Region Production and Purification

Wild-type pro region was expressed in *E. coli* strain BL21(DE3)/pLysS and purified as described previously,[20] except that the 4 M urea, 200 mM sodium chloride, 10 mM

citrate, pH 4.5 wash was omitted. Pro purity was verified by denaturing SDS–PAGE.

Pro-catalyzed Refolding

Catalyzed refolding experiments were performed as described,[20] maintaining a 16-fold excess of Pro. The biphasic refolding progress curves ([Pro] from 5 to 55 μM) were fit to a five-parameter double exponential to determine the relative contribution of each rate constant to the overall folding process. The amplitudes of the two phases were then fixed at the consensus ratio of 70/30 (fast phase/slow phase), determined from the five-parameter double exponential fit, and the data were refit to a three-parameter double exponential.[19,20,36] The rate constants for the fast phase as a function of Pro concentration were fit to a variant of the Michaelis-Menten equation[19,20] to determine k_{cat} and K_M. The rate constants for the slow phase were averaged to determine k'_{cat}, and k_i was calculated from the equality of the ratios of the fast phase to the slow phase and k_i to k_{cat}.

Pro Inhibition of $\alpha LP_{\beta\text{-turn}}$ Activity

The affinity of Pro for the native state of $\alpha LP_{\beta\text{-turn}}$ was determined from its ability to competitively inhibit $\alpha LP_{\beta\text{-turn}}$ proteolytic activity as described previously.[19,36] The apparent K_i was determined from a fit of the data to the tight-binding inhibitor equation.[6,19]

Uncatalyzed Refolding

The spontaneous refolding of $\alpha LP_{\beta\text{-turn}}$ (3 μM) and WT αLP (3 μM) were assayed as described previously.[20] The rate constant (k_f) was determined from a linear fit of the fraction of $\alpha LP_{\beta\text{-turn}}$ or WT αLP refolded as a function of time.

Unfolding

Unfolding experiments were carried out as described previously,[37] except the reactions contained 1.5 μM $\alpha LP_{\beta\text{-turn}}$, and fluorescence was measured at 0°C using a Fluoromax-3 (J.Y. Horiba) with an excitation wavelength of 290 nm. Unfolding rate constants were determined from a three-parameter exponential fit of the data. The unfolding rate in the absence of denaturant (k_u) was extrapolated from a linear fit of the logarithm of the observed rate constants as a function of denaturant.

Autolysis

$\alpha LP_{\beta\text{-turn}}$ (4 μM) was incubated at 0°C in 10 mM potassium acetate, 6.32 M guanidine hydrochloride, pH 5.0 or 10 mM HEPES, 6.38 M guanidine hydrochloride, pH 7.0. The concentration of guanidine hydrochloride in each reaction was determined from refractive index measurements.[38] Loss of protease activity over time was assayed as described previously,[39] and the data were fit to a three-parameter exponential decay.

Data Analysis

All data analysis was performed using Kaleidagraph v. 3.6 (Synergy Software Technologies, Inc.).

RESULTS

Pro-catalyzed Refolding of $\alpha LP_{\beta\text{-turn}}$

Previous studies of the folding landscapes of αLP and SGPB indicate that a smaller pro region size correlates with a lower free energy of activation for folding.[7] Because the turn conformation of the conserved β-hairpin covaries with pro region size, we expected that replacing the WT αLP β-hairpin turn with that from SGPB would result in faster folding. We first characterized the pro region-catalyzed refolding of $\alpha LP_{\beta\text{-turn}}$. As with WT αLP,[5] when $\alpha LP_{\beta\text{-turn}}$ is diluted from denaturant it rapidly converts to a molten globule intermediate state (Int), with no appreciable folding to the native state (data not shown). Pro catalyzes the folding reaction, resulting in the rapid formation of the native state. As expected, the refolding progress curves display biphasic kinetics [Fig. 3(a)], described by the kinetic scheme:[19,20]

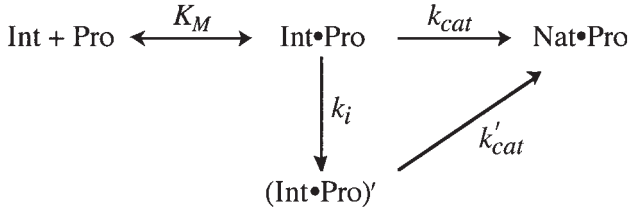

where the top line describes the fast, Pro-catalyzed folding of Int, to the native state-Pro complex (Nat · Pro), and the bottom line describes an alternate isomerization pathway. In this alternate pathway, the Michaelis complex (Int · Pro) isomerizes to an alternate (Int · Pro)′ conformation that folds more slowly than the (Int · Pro) complex.[19] The concentration dependence of the observed rate constants for the fast phase [Fig. 3(b)] reveals that the affinity of Pro for the $\alpha LP_{\beta\text{-turn}}$ intermediate state (K_M) is ~2 times tighter and the Pro-catalyzed refolding rate (k_{cat}) for $\alpha LP_{\beta\text{-turn}}$ is ~1.5 times faster compared to WT αLP (Table I). The observed rate constants for the slow phase are independent of Pro concentration [Fig. 3(c)], and they indicate that the formation of the isomerized Michaelis complex (k_i) and its slow folding to the native state (k'_{cat}) are both ~3 times faster than WT αLP (Table I).

The pro region not only catalyzes the folding reaction, but also stabilizes the native state of $\alpha LP_{\beta\text{-turn}}$ to favor the folded product. The affinity of Pro for the $\alpha LP_{\beta\text{-turn}}$ native state was assessed by Pro's ability to inhibit its proteolytic activity [Fig. 3(d)]. Pro's stabilization of the $\alpha LP_{\beta\text{-turn}}$ native state is ~3 times greater than that for WT αLP (Table I).

Spontaneous Refolding of $\alpha LP_{\beta\text{-turn}}$

Because type I′ turns are more favorable in β-hairpins than type I turns, we expected that the faster refolding of $\alpha LP_{\beta\text{-turn}}$ in the presence of Pro would extend to the uncatalyzed folding reaction. Therefore, we measured the rate of spontaneous $\alpha LP_{\beta\text{-turn}}$ refolding by monitoring the increase in folded product over time [Fig. 4(a)]. Because the spontaneous refolding is so slow, it was necessary to

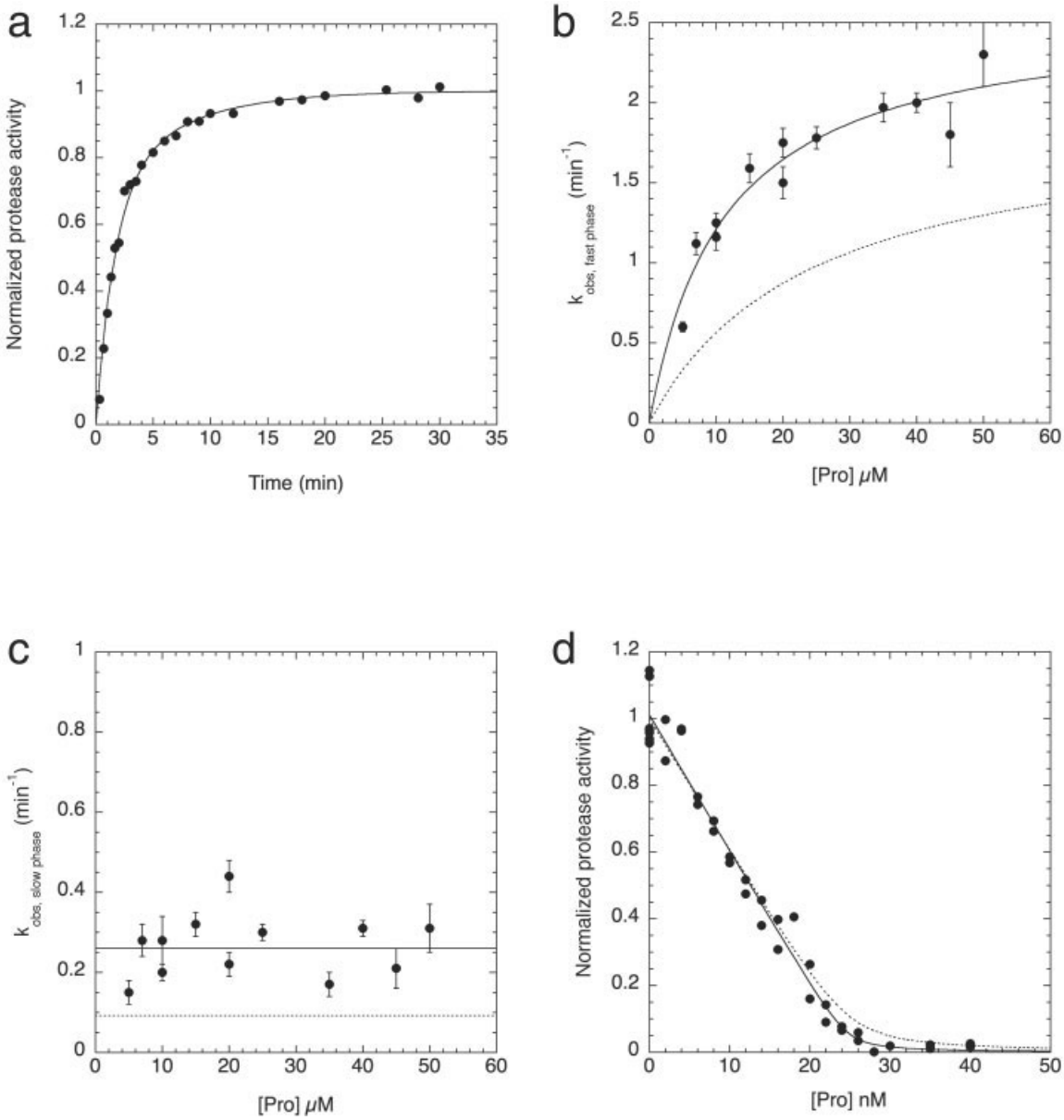

Fig. 3. Pro-catalyzed folding of $\alpha LP_{\beta\text{-turn}}$. (a) The folding of 0.31 μM $\alpha LP_{\beta\text{-turn}}$ was catalyzed by 5 μM Pro. The folding rate constants, $k_{obs,fast}$ = 0.0100 ± 0.0005 s^{-1} and $k_{obs,slow}$ = 0.0025 ± 0.0004 s^{-1}, were determined from a fit of the resulting progress curve. (**b**) The concentration dependence of the rate constants for the fast phase of Pro-catalyzed refolding of $\alpha LP_{\beta\text{-turn}}$ is well fit by a variant of the Michaelis-Menten equation[19,20] [k_{cat} = 4.3 (±0.3) × 10^{-2} s^{-1}, K_M = 11 ± 2 μM]. Error bars indicate the standard error in the fits of the refolding progress curves, as in (**a**), for each reaction. For reference purposes, the dotted line depicts the Pro-catalyzed refolding of WT αLP.[20] (**c**) The Michaelis complex isomerizes to a slow folding state [k_i = 1.8) (±0.1) × 10^{-2} s^{-1}]. The rate constants for this slow phase of Pro-catalyzed refolding of $\alpha LP_{\beta\text{-turn}}$ are independent of Pro concentration [average k'_{cat} = 4 (±1) × 10^{-3} s^{-1}, solid line]. Error bars indicate the standard error in the fits of the refolding progress curves, as in (**a**), for each reaction. The dotted line indicates the WT αLP slow phase of Pro-catalyzed refolding.[20] (**d**) $\alpha LP_{\beta\text{-turn}}$ proteolytic activity was measured in the presence of increasing amounts of Pro. The resulting tight-binding inhibition was fit to determine the affinity of Pro for the native state of $\alpha LP_{\beta\text{-turn}}$ (K_i = 0.1 ± 0.1 μM). The dotted line depicts the tight binding of Pro to the WT αLP native state.

utilize a highly sensitive peptide thiobenzyl ester substrate to measure the initial rate of the refolding reaction. Surprisingly, this analysis showed that $\alpha LP_{\beta\text{-turn}}$ spontaneously refolds at essentially the same rate as WT αLP [Fig. 4(a), Table I].

$\alpha LP_{\beta\text{-turn}}$ Unfolding

Although the slow folding and unfolding rates of $\alpha LP_{\beta\text{-turn}}$ prevent a direct measurement of its equilibrium stability, the equilibrium constant can be calculated from

TABLE I. Kinetic and Affinity Constants

	$\alpha LP_{\beta\text{-turn}}$	Wild-type αLP
k_{cat} (s^{-1})	$4.3\ (\pm 0.3) \times 10^{-2}$	$3.2\ (\pm 0.3) \times 10^{-2}$[a]
K_M (μM)	11 ± 2	24 ± 6[a]
k_i (s^{-1})	$1.8\ (\pm 0.1) \times 10^{-2}$	$5.7\ (\pm 0.5) \times 10^{-3}$[c]
k'_{cat} (s^{-1})	$4\ (\pm 1) \times 10^{-3}$	$1.53\ (\pm 0.01) \times 10^{-3}$[a]
K_i (nM)	0.1 ± 0.1	0.32 ± 0.06[b]
k_f (s^{-1})	$2.0\ (\pm 0.2) \times 10^{-11}$	$2.2\ (\pm 0.2) \times 10^{-11}$
k_u (s^{-1})	$8.3\ (\pm 0.9) \times 10^{-9}$	$2.1\ (\pm 0.2) \times 10^{-8}$[d]
ΔG_u (kcal/mol)	−3.3	−3.7

[a]Taken from Derman and Agard.[20]
[b]Taken from Peters et al.[19]
[c]A. Derman, unpublished results.
[d]Extrapolated from Jaswal et al.[37]

the ratios of the spontaneous folding and unfolding rates. Because the uncatalyzed refolding rate of $\alpha LP_{\beta\text{-turn}}$ is essentially identical to that for WT αLP, any extra stability of $\alpha LP_{\beta\text{-turn}}$ compared to WT αLP would be manifest in a slower unfolding rate. The unfolding of $\alpha LP_{\beta\text{-turn}}$ was monitored by intrinsic tryptophan fluorescence in the presence of varying concentrations of denaturant. The unfolding rate in the absence of denaturant was extrapolated from the denaturant dependent unfolding data [Fig. 4(b)] and found to be ~2.5 times slower than that for WT αLP (Table I). This corresponds to an increase in the stability of the native state by ~0.4 kcal/mol, thereby reducing the thermodynamic instability of the native state, with respect to the intermediate state, to −3.3 kcal/mol.

Kinetically stable pro-proteases gain functional longevity from their extremely cooperative unfolding behavior in which all relevant partial unfolding events are suppressed.[7,9] Therefore, we tested the cooperativity of $\alpha LP_{\beta\text{-turn}}$'s unfolding by monitoring the loss of activity over time under highly proteolytic conditions. The rate of $\alpha LP_{\beta\text{-turn}}$ autolysis [Fig. 4(c)] is the same as its unfolding rate under the same conditions. Furthermore, allowing the autolysis to proceed at a higher pH where the enzyme is more active did not accelerate the inactivation (data not shown) demonstrating that the unfolding reaction is rate limiting.

Catalytic Activity of $\alpha LP_{\beta\text{-turn}}$

Because Pro-catalyzed folding of $\alpha LP_{\beta\text{-turn}}$ is faster than that for WT αLP, and $\alpha LP_{\beta\text{-turn}}$ unfolding is slower than WT αLP, it seems surprising that WT αLP never evolved to adopt the more favorable β-hairpin turn conformation. Concerned that there might have been an impact on the catalytic efficiency of αLP's proteolytic activity, especially in light of the proximity of the β-hairpin turn to the protease active site, we measured the ability of $\alpha LP_{\beta\text{-turn}}$ to cleave a peptide substrate (Fig. 5). A Michaelis-Menten analysis of the data revealed a factor of ~11 decrease (k_{cat}/K_M) in proteolytic activity for $\alpha LP_{\beta\text{-turn}}$ compared to that of WT αLP (R. Peters, unpublished data): k_{cat} is ~3 times slower and K_M is ~3.5 times weaker.

DISCUSSION

The identification of SGPB as a closely related αLP homolog with a nearly identical native structure,[40–42] but different folding energetics[7] allows for a detailed investigation of the structural origins of their large folding and unfolding free energies of activation. Based on its conservation in pro region-containing family members and its involvement in pro region interactions, we focused on the role of the β-hairpin in αLP folding, by substituting the more favorable SGPB β-hairpin turn conformation into αLP ($\alpha LP_{\beta\text{-turn}}$).

Comparison of the folding landscapes of αLP and SGPB revealed that pro region size provides an indicator of both pro region efficacy and uncatalyzed folding energetics.[7] Because the β-hairpin turn conformation covaries with pro region size, and type I′ turns are more favorable in β-hairpins than type I turns,[24–26] we expected that the spontaneous folding of $\alpha LP_{\beta\text{-turn}}$ would be faster than that for WT αLP. Surprisingly, we found that $\alpha LP_{\beta\text{-turn}}$ and WT αLP spontaneously fold at the same rate (Table I). Instead, the unfolding rate is affected; $\alpha LP_{\beta\text{-turn}}$ unfolds ~2.5 times more slowly than WT αLP (Table I). Although this difference may be small, it corresponds to a ~0.4-kcal/mol increase in $\alpha LP_{\beta\text{-turn}}$ native state stability compared to that for WT αLP (Table I). This is comparable to the stability increase observed for favorable turn conformations in isolated β-hairpin peptides.[25,26] Furthermore, this effect of the β-turn mutation on kinetic stability is comparable in magnitude to the observed differences in kinetic stability between WT αLP and SGPB at physiological temperatures.[7]

Comparison of the spontaneous folding and unfolding rates for $\alpha LP_{\beta\text{-turn}}$ and WT αLP provides evidence for two potential models for αLP folding. The spontaneous folding rate for $\alpha LP_{\beta\text{-turn}}$ is the same as that for WT αLP, but the unfolding rate for $\alpha LP_{\beta\text{-turn}}$ is ~2.5 times faster than that for WT αLP (Table I). These data suggest that the β-hairpin is formed late in the folding reaction. However, because $\alpha LP_{\beta\text{-turn}}$ involves multiple substitutions, the folding and unfolding rates of this variant could report on either the formation of the β-hairpin or on interactions between the β-hairpin and the rest of the protein. Therefore, our data are also consistent with an alternative model where the β-hairpin may be formed early in the folding reaction, but its tight packing with a loop in an antiparallel β-sheet in the N-terminal domain of the protease (Fig. 2) may happen late in the folding reaction and be the most kinetically relevant process.

Because it was suggested that the αLP folding pathways with and without Pro catalysis share a remarkably similar folding transition state,[20] the Pro-catalyzed folding of $\alpha LP_{\beta\text{-turn}}$ may provide the means to distinguish between these two models for the role of the β-hairpin. The affinities of Pro for the folding transition state and the native state of $\alpha LP_{\beta\text{-turn}}$ are both ~3 times greater than those found for WT αLP. Additionally, the isomerization of the Michaelis complex and its subsequent slow conversion to the native state are also ~3 times faster than found for WT αLP (Table I). Together,

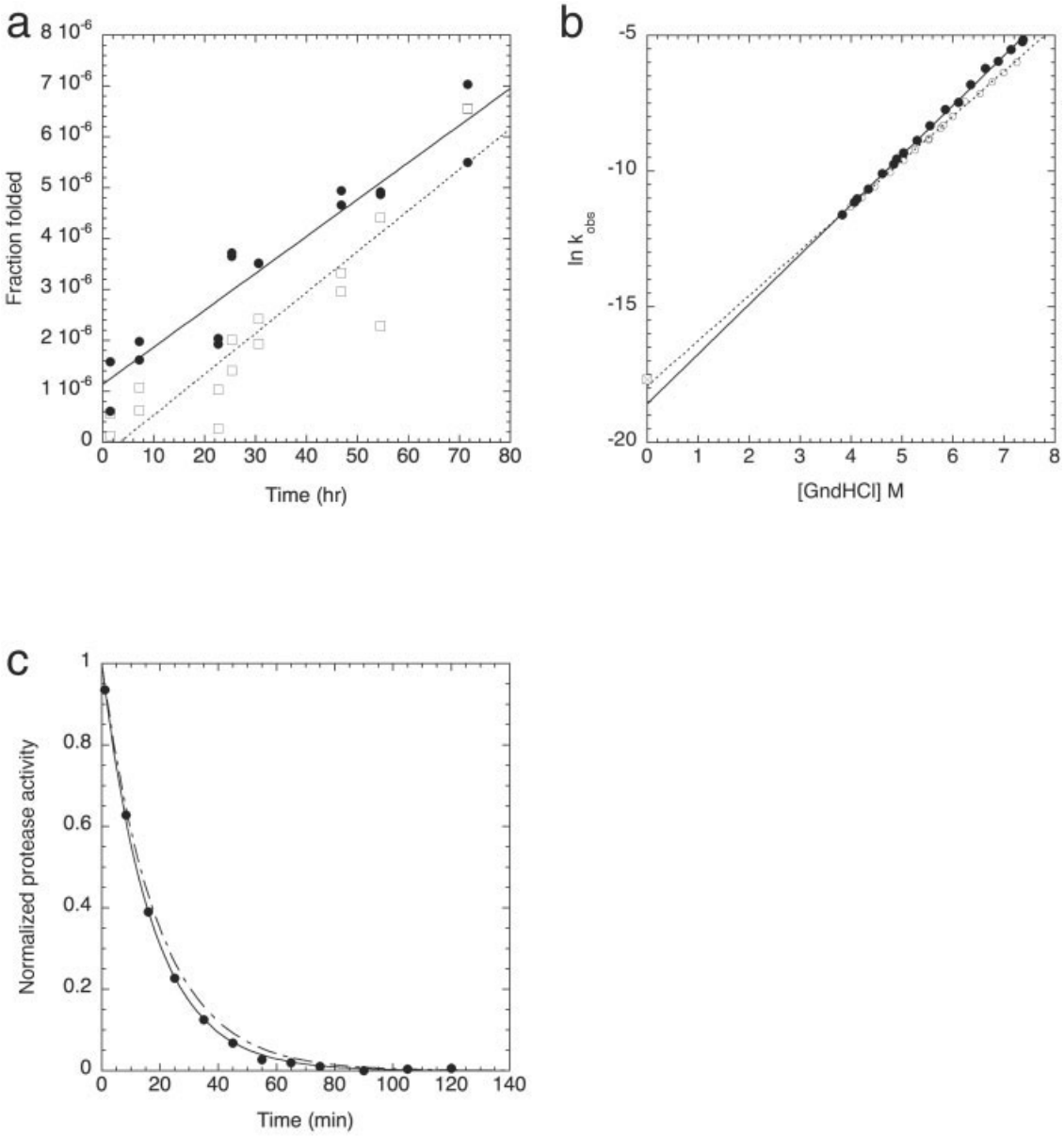

Fig. 4. $\alpha LP_{\beta\text{-turn}}$ folding and unfolding rates. (**a**) The rate of uncatalyzed folding of $\alpha LP_{\beta\text{-turn}}$ and WT αLP were calculated from linear fits of the fraction folded as a function of time [$\alpha LP_{\beta\text{-turn}}$ $k_f = 2.0\ (\pm 0.2) \times 10^{-11}$ s^{-1},WT αLP $k_f = 2.2\ (\pm 0.2) \times 10^{-11}\ s^{-1}$]. (**b**) Unfolding of $\alpha LP_{\beta\text{-turn}}$ was measured in the presence of various concentrations of denaturant. Linear extrapolation of the observed unfolding rate constants yielded the unfolding rate in the absence of denaturant [$k_u = 8.3\ (\pm 0.9) \times 10^{-9}\ s^{-1}$]. Previously measured denaturant dependent WT αLP unfolding rate constants are shown as open circles and the linear extrapolation of these data is shown as a dotted line.[4] Although those data were measured at 4°C, using an analysis of the complete temperature dependence of WT αLP unfolding,[37] it is possible to extrapolate the unfolding rate constant at 0°C, which is shown as an open square. (**c**) The rate of $\alpha LP_{\beta\text{-turn}}$ autolysis in 6.32 M denaturant was determined by monitoring the loss of active protease over time [$k_{autolysis} = 9.8\ (\pm 0.1) \times 10^{-4}\ s^{-1}$]. The autolysis of $\alpha LP_{\beta\text{-turn}}$ occurs at approximately the same rate as the global unfolding of the protease under the same buffer conditions, extrapolated from (**b**) and shown by a dashed line ($k_{obs} = 8.8\ (\pm 9.7) \times 10^{-4}\ s^{-1}$). This demonstrates that unfolding, rather than proteolysis, is rate limiting.

these data suggest that the β-hairpin is formed early in the folding reaction, because the Pro-transition state and Pro-native state interactions are enhanced to the same degree in $\alpha LP_{\beta\text{-turn}}$ compared to WT αLP. What then is the structural basis for the enhanced Pro interactions observed with $\alpha LP_{\beta\text{-turn}}$? Overlaying the crystal structures of the complex of WT αLP bound to Pro[18] and the unbound SGPB[42] suggest that these tighter interactions may result from the A127V substitution, which could alter packing with W119 in the C-terminal domain of the pro region [Fig. 2(b)]. The Val in the aligned SGPB β-hairpin is ~4.5 Å from the Trp in the pro region,

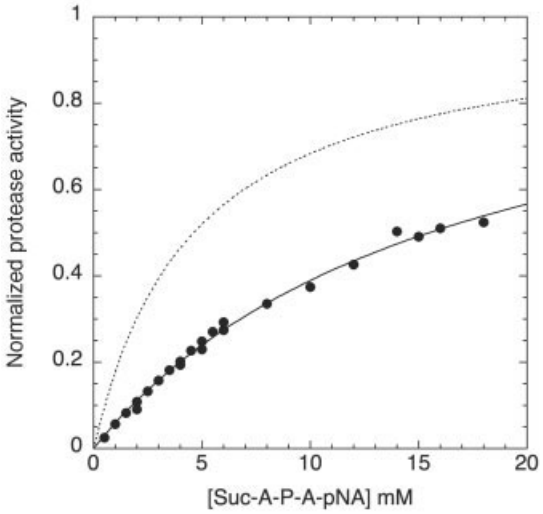

Fig. 5. $\alpha LP_{\beta\text{-turn}}$ substrate cleavage activity. The concentration dependence of the substrate cleavage activity of $\alpha LP_{\beta\text{-turn}}$ was fit to the Michaelis-Menten equation to determine the enzymatic parameters, $k_{cat} = 31 \pm 1\ s^{-1}$ and $K_M = 17 \pm 1$ mM. This corresponds to a factor of ~11 decrease in catalytic efficiency compared to WT αLP (k_{cat}/K_M = 19,400 $M^{-1}\ s^{-1}$) (R. Peters, unpublished data), which is illustrated by the dotted line.

suggesting that it could form a favorable interaction in the Pro-$\alpha LP_{\beta\text{-turn}}$ complex.

Because the β-hairpin appears to be formed early, it is likely that the precise packing of the β-hairpin with the loop in the N-terminal domain of the protease (Fig. 2) forms late in the folding reaction, contributing to the kinetic stability of the protease. Specifically, the Asp residue in the $\alpha LP_{\beta\text{-turn}}$ variant may enhance the β-hairpin's affinity for the loop in the N-terminal domain. The Asp C_β in the aligned SGPB β-hairpin is ~4 Å from αLP residues F59 and P60 [Fig. 2(b)], indicating that the G126D substitution could enhance interactions with these residues. Thus, the tight packing of the β-hairpin with the loop in the N-terminal domain of the protease appears to be important for enhancing the kinetic stability of $\alpha LP_{\beta\text{-turn}}$ beyond that for WT αLP. Moreover, this would suggest that these crossdomain interactions occur after the formation of the rate-limiting folding transition state.

Tight packing occurring throughout the protease appears to be a hallmark of the αLP native state, and is believed to be a crucial determinant of its remarkable protease resistance.[9,43] The ultrahigh resolution crystal structure of αLP revealed such a high degree of packing that a Phe in the core of the C-terminal domain is actually distorted from planarity.[40] Hydrogen-deuterium exchange experiments demonstrated that αLP has extremely large protection factors spread throughout the entire protein,[9] and not localized to a small core, as is typical for most proteins.[44] Our study suggests that optimizing the packing of substructures, especially in the domain interface, can significantly enhance the kinetic stability of the protease.

αLP has been optimized through evolution to have extremely slow unfolding that limits its susceptibility to exogenous proteolysis. However, the costs of these unique native-state properties are dramatic reductions in the rate of spontaneous folding and native-state thermodynamic stability, and they have necessitated the coevolution of its pro region folding catalyst.[7] Because $\alpha LP_{\beta\text{-turn}}$ has even slower unfolding and faster Pro-catalyzed folding than WT αLP, it seems surprising that αLP did not evolve a more favorable β-hairpin turn conformation. We find that $\alpha LP_{\beta\text{-turn}}$ has significantly impaired proteolytic activity that negates the benefits of the β-hairpin conformation for folding (Fig. 5). Intriguingly, although αLP and SGPB have different substrate specificities, preventing a direct comparison of their catalytic efficiencies, the αLP k_{cat} for substrate cleavage is ~3 times faster than that for SGPB (R. Peters, unpublished data and ref. 45). SGPB and SGPC both have the same substrate specificity, but differ in their pro region folding catalysts. The proteolytic efficiency of SGPC, which is synthesized with a long pro region, is ~3 times faster than that for SGPB.[45] Therefore, this evolutionary trade-off between folding and proteolytic activity may be quite general. The acceleration of the pro region-catalyzed folding pathway from the more favorable β-turn conformation may be more critical for proteases synthesized with less effective short pro regions, thus balancing the penalty in proteolytic activity.

The role of the β-hairpin in enhancing the kinetic stability of $\alpha LP_{\beta\text{-turn}}$, but reducing $\alpha LP_{\beta\text{-turn}}$'s proteolytic activity, appears to delineate the limitations imposed by the concurrent evolution of folding and functional properties. αLP has optimized both its folding and its native-state properties to a remarkable degree due to the decoupling of its folding and functional landscapes through the transient association of Pro. As a result, αLP is able to suppress partial unfolding events to achieve increased resistance to exogenous proteolysis, even though this is accompanied by enormous costs in folding and stability. This optimization is even seen in a thermodynamic analysis of the free energies of activation for unfolding and folding. Unlike thermodynamically stable proteins, the kinetically stable αLP and SGPB have simultaneously optimized three key parameters (the unfolding free energy of activation, the temperature of the maximum unfolding free energy of activation, and the change in heat capacity upon unfolding). Accordingly, the folding transition for αLP violates a seemingly universal behavior observed for traditional proteins.[37] Together, these data hint at the fundamental differences in composition and structure that underlay αLP's remarkable native-state properties.

Computational design and *in vitro* evolution show that, in general, the optimization of either folding or function can be extended beyond that achieved by natural evolution. Baker and coworkers demonstrated that proteins computationally redesigned in the absence of pressure for proper native-state function can fold and unfold much more rapidly than their parent proteins.[46] Bloom et al. show that function is evolved *in vitro* more efficiently when pressures on protein stability are reduced.[47] These examples demonstrate the complex limitations imposed by the concurrent evolution of folding and functional proper-

ties. αLP has achieved remarkable optimization of its native-state properties by decoupling its folding and functional landscapes through its transiently associated pro region folding catalyst. However, the $\alpha LP_{\beta\text{-turn}}$ variant, with its faster catalyzed folding and enhanced kinetic stability, but lower proteolytic efficiency, demonstrates that some limitations imposed by this evolutionary balance still remain.

CONCLUSION

Characterization of the folding landscape of a variant of αLP with a more favorable turn conformation begins to elucidate the mechanism by which αLP attains its extreme kinetic stability. Remarkably, the altered β-hairpin of $\alpha LP_{\beta\text{-turn}}$ selectively enhances the kinetic stability of the protease: it increases the free energy of activation for unfolding, while the free energy of activation for folding remains unchanged. Despite this potential advantage, this variant was not naturally selected for due to its reduced proteolytic activity. Our analysis shows that increasing tight packing of substructures within the protease, particularly at the domain interface, can have a significant impact on the kinetic stability of the protein. Moreover, it highlights the evolutionary restrictions imposed by the need to simultaneously optimize folding and functional properties.

ACKNOWLEDGMENTS

We thank B. Kelch, A. Shiau, L. Rice, J. Lyle, and E. Cunningham for many helpful discussions.

REFERENCES

1. Baker D, Shiau AK, Agard DA. The role of pro regions in protein folding. Curr Opin Cell Biol 1993;5:966–970.
2. Bryan PN. Prodomains and protein folding catalysis. Chem Rev 2002;102:4805–4816.
3. Serkina AV, Shevelev AB, Chestukhina GG. Structure and functions of bacterial proteinase precursors. Bioorg Khim 2001;27:323–346.
4. Sohl JL, Jaswal SS, Agard DA. Unfolded conformations of α-lytic protease are more stable than its native state. Nature 1998;395:817–819.
5. Baker D, Sohl JL, Agard DA. A protein-folding reaction under kinetic control. Nature 1992;356:263–265.
6. Baker D, Silen JL, Agard DA. Protease pro region required for folding is a potent inhibitor of the mature enzyme. Proteins 1992;12:339–344.
7. Truhlar SME, Cunningham EL, Agard DA. The folding landscape of Streptomyces griseus protease B reveals the energetic costs and benefits associated with evolving kinetic stability. Protein Sci 2004;13:381–390.
8. Cunningham EL, Agard DA. Disabling the folding catalyst is the last critical step in α-lytic protease folding. Protein Sci 2004;13:325–331.
9. Jaswal SS, Sohl JL, Davis JH, Agard DA. Energetic landscape of α-lytic protease optimizes longevity through kinetic stability. Nature 2002;415:343–346.
10. Fontana A, De Laureto PP, Spolaore B, Frare E, Picotti P, Zambonin M. Probing protein structure by limited proteolysis. Acta Biochim Pol 2004;51:299–321.
11. Fontana A, Polverino de Laureto P, De Filippis V, Scaramella E, Zambonin M. Probing the partly folded states of proteins by limited proteolysis. Fold Des 1997;2:R17–R26.
12. Imoto T, Yamada H, Ueda T. Unfolding rates of globular proteins determined by kinetics of proteolysis. J Mol Biol 1986;190:647–649.
13. Hubbard SJ. The structural aspects of limited proteolysis of native proteins. Biochim Biophys Acta 1998;1382:191–206.
14. Bai Y, Sosnick TR, Mayne L, Englander SW. Protein folding intermediates: native-state hydrogen exchange. Science 1995;269:192–197.
15. Chamberlain AK, Handel TM, Marqusee S. Detection of rare partially folded molecules in equilibrium with the native conformation of RNaseH. Nat Struct Biol 1996;3:782–787.
16. Kim PS, Baldwin RL. Intermediates in the folding reactions of small proteins. Annu Rev Biochem 1990;59:631–660.
17. Zajicek JL, Carter RM, Ghiron CA. A spectroscopic analysis of the thermally induced folding-unfolding transition of beta-trypsin. Biophys J 1981;35:23–29.
18. Sauter NK, Mau T, Rader SD, Agard DA. Structure of α-lytic protease complexed with its pro region. Nat Struct Biol 1998;5:945–950.
19. Peters RJ, Shiau AK, Sohl JL, Anderson DE, Tang G, Silen JL, Agard DA. Pro region C-terminus: protease active site interactions are critical in catalyzing the folding of α-lytic protease. Biochemistry 1998;37:12058–12067.
20. Derman AI, Agard DA. Two energetically disparate folding pathways of α-lytic protease share a single transition state. Nat Struct Biol 2000;7:394–397.
21. Sibanda BL, Blundell TL, Thornton JM. Conformation of beta-hairpins in protein structures. A systematic classification with applications to modelling by homology, electron density fitting and protein engineering. J Mol Biol 1989;206:759–777.
22. Sibanda BL, Thornton JM. Beta-hairpin families in globular proteins. Nature 1985;316:170–174.
23. Chothia C. Conformation of twisted beta-pleated sheets in proteins. J Mol Biol 1973;75:295–302.
24. Kuhlman B, O'Neill JW, Kim DE, Zhang KY, Baker D. Accurate computer-based design of a new backbone conformation in the second turn of protein L. J Mol Biol 2002;315:471–477.
25. Santiveri CM, Santoro J, Rico M, Jimenez MA. Factors involved in the stability of isolated beta-sheets: Turn sequence, beta-sheet twisting, and hydrophobic surface burial. Protein Sci 2004;13:1134–1147.
26. Cochran AG, Tong RT, Starovasnik MA, Park EJ, McDowell RS, Theaker JE, Skelton NJ. A minimal peptide scaffold for beta-turn display: optimizing a strand position in disulfide-cyclized beta-hairpins. J Am Chem Soc 2001;123:625–632.
27. Silen JL, McGrath CN, Smith KR, Agard DA. Molecular analysis of the gene encoding alpha-lytic protease: evidence for a preproenzyme. Gene 1988;69:237–244.
28. Henderson G, Krygsman P, Liu CJ, Davey CC, Malek LT. Characterization and structure of genes for proteases A and B from Streptomyces griseus. J Bacteriol 1987;169:3778–3784.
29. Cunningham EL, Agard DA. Interdependent folding of the N- and C-terminal domains defines the cooperative folding of α-lytic protease. Biochemistry 2003;42:13212–13219.
30. Hunkapiller MW, Smallcombe SH, Whitaker DR, Richards JH. Carbon nuclear magnetic resonance studies of the histidine residue in alpha-lytic protease. Implications for the catalytic mechanism of serine proteases. Biochemistry 1973;12:4732–4743.
31. Mace JE, Agard DA. Kinetic and structural characterization of mutations of glycine 216 in α-lytic protease: a new target for engineering substrate specificity. J Mol Biol 1995;254:720–736.
32. Sadler JR, Tecklenburg M, Betz JL. Plasmids containing many tandem copies of a synthetic lactose operator. Gene 1980;8:279–300.
33. Mace JE, Wilk BJ, Agard DA. Functional linkage between the active site of α-lytic protease and distant regions of structure: scanning alanine mutagenesis of a surface loop affects activity and substrate specificity. J Mol Biol 1995;251:116–134.
34. Bradford MM. A rapid and sensitive method for the quantitation of microgram quantities of protein utilizing the principle of protein-dye binding. Anal Biochem 1976;72:248–254.
35. Spector T. Refinement of the Coomassie blue method of protein quantitation. Anal Biochem 1978;86:142–146.
36. Cunningham EL, Mau T, Truhlar SM, Agard DA. The pro region N-terminal domain provides specific interactions required for catalysis of alpha-lytic protease folding. Biochemistry 2002;41:8860–8867.
37. Jaswal SS, Truhlar SME, Dill KA, Agard DA. Comprehensive analysis of protein folding activation thermodynamics reveals a universal behavior violated by kinetically stable proteases. J Mol Biol 2005;347:355–366.
38. Pace CN. Determination and analysis of urea and guanidine

hydrochloride denaturation curves. Methods Enzymol 1986;131: 266–280.
39. Silen JL, Frank D, Fujishige A, Bone R, Agard DA. Analysis of prepro-alpha-lytic protease expression in Escherichia coli reveals that the pro region is required for activity. J Bacteriol 1989;171: 1320–1325.
40. Fuhrmann CN, Kelch BA, Ota N, Agard DA. The 0.83 A resolution crystal structure of alpha-lytic protease reveals the detailed structure of the active site and identifies a source of conformational strain. J Mol Biol 2004;338:999–1013.
41. Fujinaga M, Delbaere LT, Brayer GD, James MN. Refined structure of alpha-lytic protease at 1.7 A resolution. Analysis of hydrogen bonding and solvent structure. J Mol Biol 1985;184:479–502.
42. Read RJ, Fujinaga M, Sielecki AR, James MN. Structure of the complex of Streptomyces griseus protease B and the third domain of the turkey ovomucoid inhibitor at 1.8-A resolution. Biochemistry 1983;22:4420–4433.
43. Cunningham EL, Jaswal SS, Sohl JL, Agard DA. Kinetic stability as a mechanism for protease longevity. Proc Natl Acad Sci USA 1999;96:11008–11014.
44. Li R, Woodward C. The hydrogen exchange core and protein folding. Protein Sci 1999;8:1571–1590.
45. Sidhu SS, Kalmar GB, Willis LG, Borgford TJ. Streptomyces griseus protease C. A novel enzyme of the chymotrypsin superfamily. J Biol Chem 1994;269:20167–20171.
46. Kuhlman B, Baker D. Exploring folding free energy landscapes using computational protein design. Curr Opin Struct Biol 2004; 14:89–95.
47. Bloom JD, Wilke CO, Arnold FH, Adami C. Stability and the evolvability of function in a model protein. Biophys J 2004;86:2758–2764.
48. Glasstone S, Laidler, K., and Eyring, H. The theory of rate processes: the kinetics of chemical reactions, viscosity, diffusion, and electrochemical phenomena. New York: McGraw-Hill Book Company, Inc.; 1941.
49. DeLano WL. The PyMOL molecular graphics system. San Carlos, CA: DeLano Scientific; 2002.